Wavelength dependence four-wave mixing spectroscopy in a micrometric atomic vapour*

Li Yuan-Yuan(李院院)[a)b)†], Li Li(李 莉)[a)], Zhang Yan-Peng(张彦鹏)[c)], and Bi Si-Wen(毕思文)[b)]

[a)] *Institute of Optics & Electronics, Department of Physics, Xi'an University of Arts and Science, Xi'an* 710065, *China*
[b)] *State Key Laboratory of Transient Optics and Technology, Xi'an Institute of Optics and Precision Mechanics, Chinese Academy of Sciences, Xi'an* 710068, *China*
[c)] *Key Laboratory for Physical Electronics and Devices of the Ministry of Education, Xi'an Jiaotong University, Xi'an* 710049, *China*

(Received 28 January 2010; revised manuscript received 9 March 2010)

This paper presents a theoretical study of wavelength dependence four-wave-mixing (FWM) spectroscopy in a micrometric thin atomic vapour. It compares three cases termed as mismatched case I, matched case and mismatched case II for the probe wavelength less, equal and greater than the pump wavelength respectively. It finds that Dicke-narrowing can overcome width broadening induced by Doppler effects and polarisation interference of thermal atoms, and high resolution FWM spectra can be achieved both in matched and mismatched wavelength for many cases. It also finds that the magnitude of the FWM signal can be dramatically modified to be suppressed or to be enhanced in comparison with that of matched wavelength in mismatched case I or II. The width narrowing and the magnitude suppression or enhancement can be demonstrated by considering enhanced contribution of slow atoms induced by atom-wall collision and transient effect of atom-light interaction in a micrometric thin vapour.

Keywords: four-wave mixing, wavelength match, Dicke-narrowing, polarisation interference
PACC: 0765, 6800

1. Introduction

It has been reported in early days that frequent atom–wall collisions can overcome the effects of optical pumping when atomic vapours are contained in thin cells, as a result enhanced degenerate four-wave mixing (FWM) signals are observed at noncycling transitions.[1] Thin vapour cells have also been extensively used in the observation of sub-Doppler spectral lines by several authors.[2−5] This narrowing structure spectrum in a thin cell is mainly from transient effects induced by atom–wall collisions.[2−5] On the other hand, in a macroscopic cell the best electromagnetically induced transparency (EIT) can be achieved for mismatched wavelengths.[6] It has also been shown that the FWM signal can be largely enhanced due to the suppression of absorptive photons.[7,8] However, polarisation interference from different ensembles of atoms can cause significant modification of the non-degenerate FWM spectra, and lead to a width broadening in a cascade three-level system in a macroscopic cell.[9] Is it possible to overcome the width broadening of the FWM spectra induced by Doppler effects and polarisation interference in a micrometric vapour?

Motivated by these works, we present a theoretical model in this paper for investigating wavelength dependence FWM spectroscopy in a cascade three-level atomic system (Fig. 1(b)) in a micrometric thin vapour. The thickness of the micrometric vapour (e.g., a typical value of 10 μm) satisfies $\langle v\rangle\tau_{\rm p} \geq L \geq \langle v\rangle\Gamma^{-1}$ with $\langle v\rangle$, $\tau_{\rm p}$ and Γ^{-1} the mean thermal velocity, the optical pumping time and the excited state lifetime respectively, the atom–light interaction time is long compared to the excited state decay and several absorption emission cycles can take place.[10] However, the optical pumping efficiency is strongly dependent on the atomic velocity and only the slowest atoms may approach a steady state.[10] Thus very narrow spectra of FWM can be achieved due to atom-wall collision in such a confined atomic system.

In a phase-conjugated beam configuration (Fig. 1(a)) applied to a cascade three-level atomic system (Fig. 1(b)), we denote λ_1 and $\lambda_2(\lambda_2' = \lambda_2)$ as wavelengths of the probe and the pump beams

*Project supported from the Major Program of Science Foundation of Xi'an University of Arts and Science.
†Corresponding author. E-mail: liyynxcn@yahoo.com.cn
© 2010 Chinese Physical Society and IOP Publishing Ltd

1 and 2(3) respectively. Three wavelength regimes are considered: mismatched wavelengths for which the probe wavelength is less than the pump wavelength ($\lambda_1 < \lambda_2$) (mismatched case I); matched wavelengths for which the probe wavelength and the pump wavelength are equal ($\lambda_1 = \lambda_2$) (matched case); mismatched wavelengths for which the probe wavelength is greater than the pump wavelength ($\lambda_1 > \lambda_2$) (mismatched case II).[6]

Our main discovery of this work is that Dicke-narrowing FWM spectra can be realized both in matched and mismatched regimes, while the magnitude of FWM signal can be dramatically suppressed or enhanced by selecting mismatched case I or II respectively. It is feasible to achieve high resolution FWM spectroscopy as well as high efficient FWM signals with thin vapour cells, which may have some possible applications in optical information processing and the design of full optical devices.

2. Theoretical model

We consider a cascade three-level atomic system in a thin vapour presented in Fig. 1(b), where $|0\rangle$, $|1\rangle$ and $|2\rangle$ represent the ground, the intermediate and the excited states respectively. Transition frequencies of $|0\rangle - |1\rangle$ and $|1\rangle - |2\rangle$ are Ω_1 and Ω_2 respectively. Three laser beams are applied to the system (Fig. 1(a)), where beam 1 represents the probe field ε_1, beams 2 and 3 propagating with a small angle difference (about 0.5°) consist of coupling fields ε_2 and ε_2' respectively. The FWM signal can be generated and propagates almost opposite to the beam 3 if the phase-matching condition $k_F = k_1 + k_2 - k_2'$ is satisfied, where $k_i(k_i')$ is the wave vector of the field $\varepsilon_i(\varepsilon_i')$ ($i = 1, 2$).

It is assumed that the Fabry–Perot effect can be neglected if two windows of the cells are antireflection coated, since the intensity of the back reflection beam in a micrometric thin vapour is much smaller than that of the forward beam.[11] When we consider the polarisation interference induced by different ensembles of atoms, the intensity of the FWM signal is proportional to $|\int_0^L P(z)\mathrm{d}z|^2$, where $P(z)$ is the local nonlinear polarisation, L is the thickness of the thin vapour. If the Doppler effects is involved, and the velocity of thermal atoms is assumed to obey the Maxwell distribution $W(v) = (u\sqrt{\pi})^{-1}\exp(-v^2/u^2)$ with u being the probable velocity, the nonlinear polarisation can be calculated by

$$P(z) = N\mu_{10}\int_{-\infty}^{\infty} W(v)\sigma_{10}^{(3)}(t)\mathrm{d}v, \tag{1}$$

where N is the density of atoms, μ_{10} is the dipole moment matrix element, $\sigma_{10}^{(3)}$ is the third-order density matrix element.

Next, we calculate $\sigma_{10}^{(3)}$ by the process

$$\sigma_{00}^{(0)} \xrightarrow{\omega_1} \sigma_{10}^{(1)} \xrightarrow{\omega_2} \sigma_{20}^{(2)} \xrightarrow{-\omega_2} \sigma_{10}^{(3)}, \quad \text{(P)}$$

and following coupling equations:

$$\partial\sigma_{10}^{(1)}/\partial t = -\Lambda_{10}\sigma_{10}^{(1)} + \mathrm{i}\, g_1, \tag{2}$$

$$\partial\sigma_{20}^{(2)}/\partial t = -\Lambda_{20}\sigma_{20}^{(2)} + \mathrm{i}\, g_2\sigma_{10}^{(1)}, \tag{3}$$

$$\partial\sigma_{10}^{(3)}/\partial t = -\Lambda_{10}\sigma_{10}^{(3)} + \mathrm{i}\, g_2'\sigma_{20}^{(2)}, \tag{4}$$

where the Doppler-shifted detunings are defined as $\Lambda_{10} = \Gamma_{10} + \mathrm{i}(k_1 v + \Delta_1)$, $\Lambda_{20} = \Gamma_{20} + \mathrm{i}(k_1 v + k_2 v + \Delta_1 + \Delta_2)$, in which Γ_{10} and Γ_{20} are the decay rate from level $|1\rangle$ to $|0\rangle$ and the dephasing rate between level $|2\rangle$ and $|0\rangle$ respectively, the detuning of the field ε_i (ε_i') is defined as $\Delta_i = \Omega_i - \omega_i$ ($i = 1, 2$) respectively. Rabi frequencies g_1, g_2 and g_2' are defined as $g_1 = \mu_{10}\varepsilon_1/\hbar$, $g_2 = \mu_{21}\varepsilon_2/\hbar$ and $g_2' = \mu_{21}\varepsilon_2'/\hbar$ respectively.

To write down the coupling equations (2)–(4), the coherence σ_{21} is neglected, this is justified for two reasons, one is that in a steady state σ_{21} is much less than σ_{10} and σ_{20}, the other is that the factor before this term is the Rabi frequency g_1 of the weak probe field.

It is assumed that the initial conditions for the equations (2)–(4) are $\sigma_{00} = 1$, $\sigma_{11} = 0$ and $\sigma_{i0}(t = 0) = 0$ ($i = 1, 2$). We then solve the process (P) and the coupling equations (2)–(4), and a Laplace transformed solution of the density matrix element $\sigma_{10}^{(3)}$ yields

$$\sigma_{10}^{(3)}(s) = -\mathrm{i}\, g_1 g_2 g_2'/[s(s+\Lambda_{10})^2(s+\Lambda_{20})]. \tag{5}$$

After applying inverse-Laplace transform to the above equation, we immediately obtain the expression of $\sigma_{10}^{(3)}$ as a function of atom–light interaction time of t

$$\begin{aligned}\sigma_{10}^{(3)}(t) = &-\mathrm{i}\, g_1 g_2 g_2'[A + B\exp(-\Lambda_{10}t) \\ &+ Ct\exp(-\Lambda_{10}t) + D\exp(-\Lambda_{20}t),\end{aligned} \tag{6}$$

where

$$A = 1/(\Lambda_{10}^2\Lambda_{20}),$$

$$B = (2\Lambda_{10} - \Lambda_{20})/[\Lambda_{10}^2(\Lambda_{10} - \Lambda_{20})^2],$$

$$C = 1/[\Lambda_{10}(\Lambda_{10} - \Lambda_{20})]$$

and

$$D = -1/[\Lambda_{20}(\Lambda_{20} - \Lambda_{10})^2].$$

We assume that atoms get de-excited at a collision with the wall, and are in the ground states at the instant that they leave the wall after a collision. Thus the atom–light interaction time for atoms with positive velocities is different from that of atoms with negative velocities, and Eq. (1) can be expressed as[12]

$$P(z) = N\mu_{10}\int_{-\infty}^{\infty} W(v)[\Theta(v)\sigma_{10}^{(3+)} + \Theta(-v)\sigma_{10}^{(3-)}]\mathrm{d}v, \tag{7}$$

where $\Theta(v)$ and $\Theta(-v)$ are Heaviside functions, $\sigma_{10}^{(3+)}$ and $\sigma_{10}^{(3-)}$ are the density matrix elements for $v > 0$ and $v < 0$ respectively.

According to above assumption, we take $t = z/v$ for $v > 0$ and $t = (z - L)/v$ for $v < 0$ in Eq. (6), then substitute into Eq. (7), and change the integration orders of v and z, we finally obtain the formula of FWM signal and expressed as

$$I_{\mathrm{FWM}} \propto |\int_{-\infty}^{+\infty} W(v)\mathrm{d}v(F_1 + F_2 + F_3)|^2, \tag{8}$$

where

$$F_1 = AL, \tag{8a}$$

$$F_2 = B|v|/\Lambda_{10} + C|v|/\Lambda_{10}^2 + D|v|/\Lambda_{20}, \tag{8b}$$

$$F_3 = -B|v|/\Lambda_{10}\exp(-\Lambda_{10}L/|v|) - C(|v| + \Lambda_{10}L)/\Lambda_{10}^2\exp(-\Lambda_{10}L/|v|) - D|v|/\Lambda_{20}\exp(-\Lambda_{20}L/|v|). \tag{8c}$$

The form of the formula (8) is similar to that of previous discussion.[12–14] The first term in Eq. (8) represents a usual steady-state FWM spectra in a free space. Dicke-narrowing features are associated with the transient effects as considered in the second and the third terms, which respectively illustrate the integration of all possible interaction inside the medium and the confining features of the interaction time $L/|v|$.

3. Results and discussion

We consider a micrometric vapour cell with a typical thickness of 10 μm. For a general comparison of different wavelength regimes, it would not be possible to study a real atomic system. Similar to Ref. [6], the wavelength of the probe field is kept constant while three values are selected for the pump fields. The wavelength of the probe field is taken to be 800 nm, and the wavelength of the pump fields is selected to be 1600 nm, 800 nm and 400 nm respectively for the mismatched case I ($\lambda_1 < \lambda_2$), the matched case ($\lambda_1 = \lambda_2$) and the mismatched case II ($\lambda_1 > \lambda_2$). The wave vector is taken as $k_1 > 0$ and $k_2 < 0$ for our beam configuration as shown in Fig. 1(a) in our numerical calculation. We set the decay rates Γ_{10} and Γ_{20} to be 42 MHz, and the probable velocity of atoms to be 270 m/s.

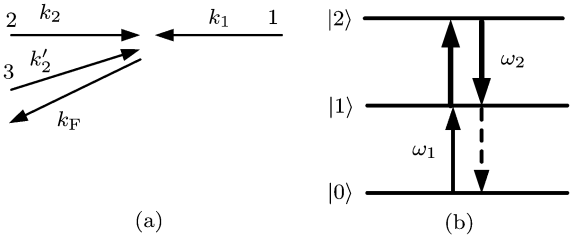


Fig. 1. Beam configuration (a) and level diagram (b) of FWM in a cascade three-level atomic system.

The predicted FWM lines versus the probe detuning are presented in Figs. 2 and 3, where solid, dashed and dotted lines respectively represent the mismatched case I, matched case and the mismatched case II. The line shape in Figs. 2 and 3 can be demonstrated by considering the magnitude of macroscopic polarisation as a function of the atomic velocity and the probe detuning. We plot contour figures in Fig. 4 to show the contribution of different ensembles of atoms with different velocities at proper probe detuning in the presence of the pump fields.

We first consider only the line shape in Fig. 2, where the signal is normalised by the maximum value of the signal for $\Delta_1 = \Delta_2 = 0$ in each case. As the pump fields are exactly detuned on the resonance to the transition to $|1\rangle - |2\rangle$ (i.e., $\Delta_2 = 0$), the FWM lines share almost the same width in three cases, and this narrowing width is about 54 MHz. This feature does not preserve in a macroscopic cell, since the contribution made by the Doppler effects and the polarisation interference leads to a width broadening. It should be noted that this broadening decreased largely due to an enhanced contribution of slow atoms induced by atom–wall collision in such a micrometric vapour (Figs. 4(a)–4(c)). However, the broadening can not be totally eliminated as the pump fields are detuned away from the exact resonance position. In these cases different ensembles of atoms with relatively greater velocities participate in atom–light interaction and introduce a broadening of the spectrum. Moreover, the width broadening is somewhat manifest for the mismatched case I (e.g., about 80 MHz for $\Delta_2 = -84$ MHz) comparing to that of two other cases, since this interference mainly suppress the centre of the line in the mismatched case I.[9]

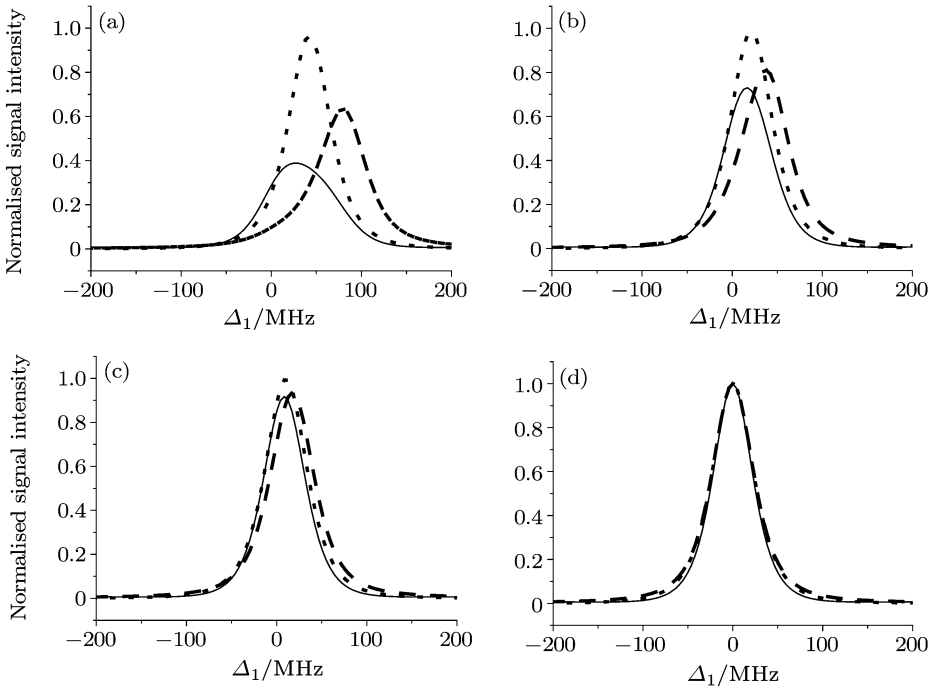


Fig. 2. Line shape of the FWM signals versus the probe detuning Δ_1 for $\lambda_2 = 1600$ nm (solid lines), 800 nm (dashed lines) and 400 nm (dotted lines) in a thin atomic vapour with a thickness of 10 μm. Other parameters are $\Delta_2 = -84$ MHz, -42 MHz, -21 MHz and 0 in (a), (b), (c) and (d) respectively. The signals for $\Delta_1 = \Delta_2 = 0$ are normalised to be 1 in each wavelength regime.

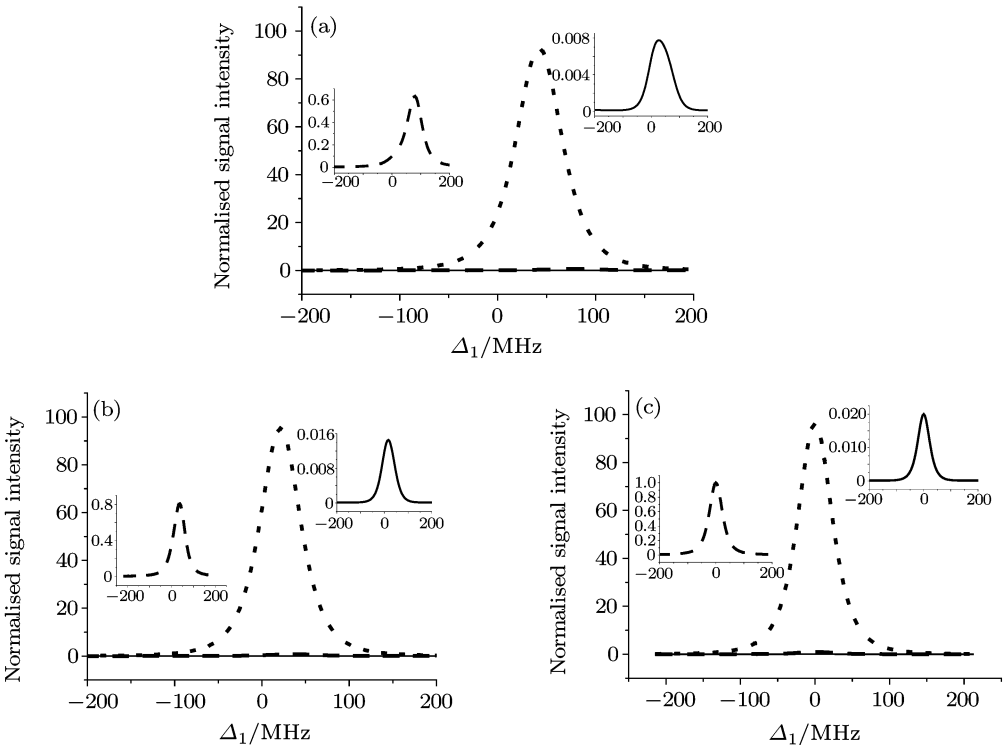


Fig. 3. Comparison of magnitude of FWM signals for $\lambda_2 = 1600$ nm (solid lines), 800 nm (dashed lines) and 400 nm (dotted lines) in a thin atomic vapour with a thickness of 10 μm. Other parameters are $\Delta_2 = -84$ MHz, -42 MHz, and 0 in (a), (b), and (c) respectively. The signal for $\lambda_2 = 800$ nm, $\Delta_1 = \Delta_2 = 0$ is normalised to be 1.

To compare the magnitude of the FWM signals for three cases, the signal is normalised by the maximum value of matched case for $\Delta_1 = \Delta_2 = 0$, and the FWM lines are plotted in Fig. 3 for $\Delta_2 = -84$ MHz, -42 MHz,

and 0 in Figs. 3(a), 3(b) and 3(c) respectively. We find that in both cases the width broadening induced by polarisation interference can be limited in such a micrometric thin vapour, all lines shape shares a Dicke-narrowing structure. Comparing to the matched case, the magnitude of the FWM signals for the mismatched cases I and II can be dramatically suppressed and enhanced respectively. The ratios of the magnitude of matched case to that of the mismatched case I and the magnitude of mismatched case II to that of the matched case can reach an order of 10^2. One reason for the suppression and the enhancement of the FWM signal is from the relatively smaller or greater absorptive reduction in an EIT regime for the mismatched cases I and II respectively.[6] The other reason is that the numbers of atoms participating in atom–light interaction is different due to different Doppler-shifted contribution from the pump fields in three cases. Since the Doppler shift from the pump fields is proportional to the frequency of the pump fields themselves, more atoms can be involved in the participation in atom–light interaction when we decrease the pump wavelength, as a result the magnitude of the FWM signal can be suppressed or enhanced for the mismatched cases I and II respectively.[6]

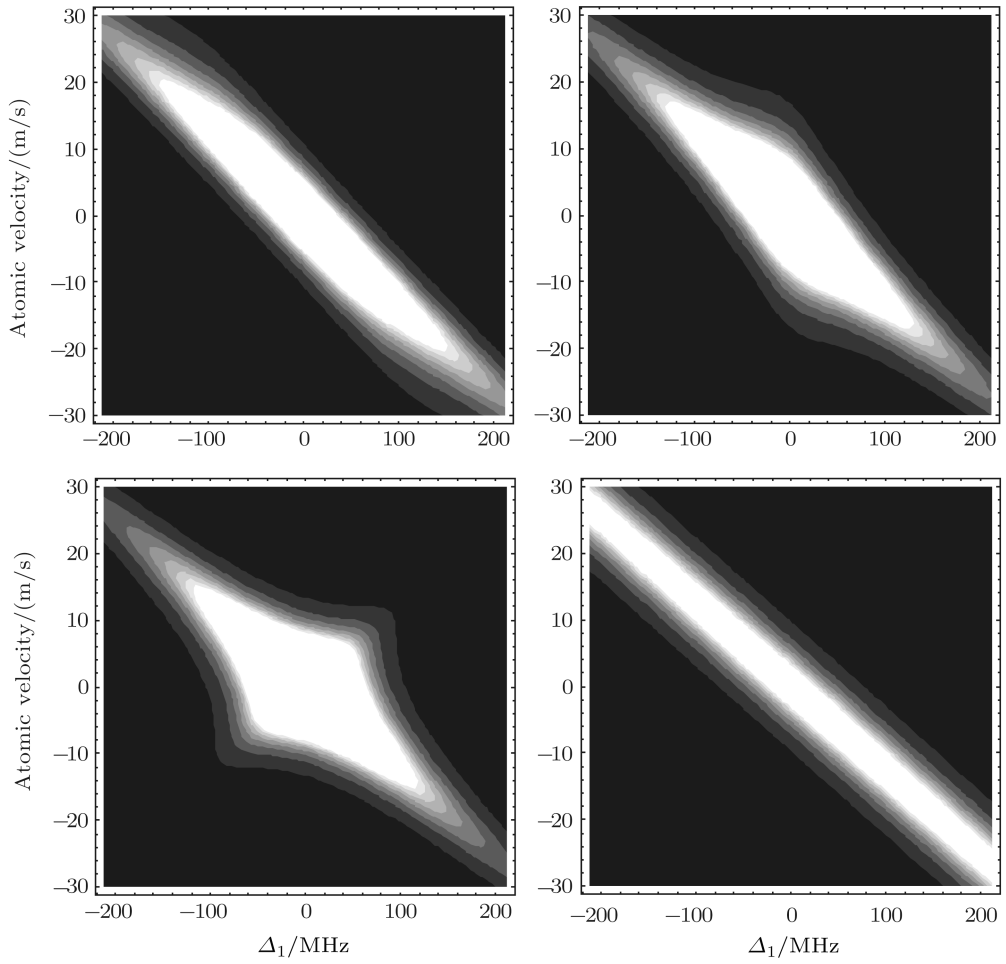


Fig. 4. Atomic velocity and the probe detuning selection in the FWM signal, (a), (b) and (c) for the mismatched case I, the matched case and the mismatched case II respectively, and (d) for both matched and mismatched cases. The detunings of λ_2 are $\Delta_2 = 0$ in (a)–(c) and -42 MHz in (d).

4. Conclusion

The FWM spectra of cascade three-level atoms confined in a 10 μm vapour is predicted for three wavelengths schemes: mismatched case I ($\lambda_1 < \lambda_2$); matched case ($\lambda_1 = \lambda_2$); mismatched case II ($\lambda_1 > \lambda_2$). We have shown that Dicke-narrowing type FWM signals can be achieved both in the matched and mismatched wavelengths regimes. However, this feature does not preserve in a macroscopic cell, since the contribution made by the Doppler effects and the polarisation interference leads to a width broadening. We would like to stress that

this broadening can be overcome by slow atoms induced by atom–wall collision in a micrometric thin vapour. We have also shown that the magnitude of the FWM signal can be dramatically modified to be suppressed (in the mismatched case I) or enhanced (in the mismatched case II) comparing to that of the matched case. This modification can be demonstrated by investigating the contribution of individual or group of atoms with particular velocities as the probe field is detuned in the presence of the pump fields. The study of this work may be employed for achieving high resolution FWM spectrum with enhanced magnitude by using thin vapour cells, which may have some possible applications in measuring atomic parameters, optical information processing and the design of full optical devices.

References

[1] Ai B, Glassner D S and Knize R J 1994 *Phys. Rev.* A **50** 3345

[2] Briaudeau S, Bloch D and Ducloy M 1996 *Europhys. Lett.* **35** 337

[3] Sarkisyan D, Varzhapetyan T, Sarkisyan A, Malakyan Yu, Papoyan A, Lezama A, Bloch D and Ducloy M 2004 *Phys. Rev.* A **69** 065802

[4] Sargsyan A, Sarkisyan D and Papoyan A 2006 *Phys. Rev.* A **73** 033803

[5] Andreeva C, Cartaleva S, Petrov L, Saltiel S, Sarkisyan D, Varzhapetyan T, Bloch D and Ducloy M 2007 *Phys. Rev.* A **76** 013837

[6] Boon J, Zekou E, McGloin D and Dunn M 1999 *Phys. Rev.* A **59** 4675

[7] Wu Y, Saldana J and Zhu Y 2003 *Phys. Rev.* A **67** 013811

[8] Zhang Y, Brown Andy W and Xiao M 2007 *Phys. Rev. Lett.* **99** 123603

[9] Zuo Z, Sun J, Liu X, Wu L and Fu P 2007 *Phys. Rev.* A **75** 023805

[10] Failache H, Lenci L, Lezama A, Bloch D and Ducloy M 2007 *Phys. Rev.* A **76** 053826

[11] Dutier G, Saltiel S, Bloch D and Ducloy M 2003 *J. Opt. Soc. Am.* B **20** 793

[12] Li Y, Bai J, Li L, Zhang W, Li C, Nie Z, Gan C and Zhang Y 2008 *Chin. Phys. Lett.* **25** 3238

[13] Li Y Y, Hou X, Bai J, Yan J F, Gan C L and Zhang Y P 2008 *Chin. Phys.* B **17** 2885

[14] Li Y Y, Zhou Y and Zhang G Z 2006 *Chin. Phys.* **15** 985